37. M. F. Kaplan and C. E. Miller, *J. Pers. Soc. Psychol.* **53**, 306 (1987); S. Tanford and S. Penrod, *J. Appl. Soc. Psychol.* **16**, 322 (1986).
38. J. Hartwick, B. H. Sheppard, J. H. Davis, in *Improving Group Decision Making in Organizations*, R. Guzzo, Ed. (Academic Press, New York, 1982), p. 41.
39. J. H. Davis, C. E. Spitzer, D. H. Nagao, G. Stasser, in *Dynamics of Group Decisions*, H. Brandstatter, J. H. Davis, H. Schuler, Eds. (Sage, Beverly Hills, CA 1978); V. P. Hans and A. N. Doob, *Criminal Law* **18**, 235 (1976).
40. Citizens' evaluations of the desirability of judges and different types of juries are examined in R. J. MacCoun and T. R. Tyler, *Law Hum. Behav.* **12**, 333 (1988).
41. C. F. Roberts, S. L. Golding, F. D. Fincham, *ibid.* **11**, 207 (1987); J. C. Savitsky and W. D. Lindblom, *J. Appl. Soc. Psychol.* **16**, 686 (1986).
42. J. C. Mowen and D. E. Linder, in *Social Psychology and Discretionary Law*, L. E. Abt and I. R. Stuart, Eds. (Van Nostrand Reinhold, New York, 1979), p. 219; N. Vidmar, *J. Pers. Soc. Psychol.*, **22**, 211 (1972).
43. K. S. Bordens and I. A. Horowitz, *Law Hum. Behav.* **9**, 339 (1985); S. Tanford, S. Penrod, R. Collins, *ibid.*, p. 319.
44. Supported by NSF grant SES-8796357 and by The RAND Corporation's Behavioral Science Department. I am grateful to L. Dair, D. Hensler, D. Kanouse, N. Kerr, B. Mittman, J. Peterson, J. Rolph, and T. Tyler for helpful comments on an earlier draft.

The Heliosphere as an Astrophysical Laboratory for Particle Acceleration

T. TERASAWA AND M. SCHOLER

Particle acceleration is one of the most important topics in plasma astrophysics as well as in cosmic-ray astrophysics. The heliosphere is an ideal astrophysical laboratory, wherein one can observe in situ the elementary mechanisms involved in the particle acceleration processes. Two phenomena of special interest are stochastic acceleration in the magnetohydrodynamic turbulence around comets and stochastic shock acceleration at interplanetary shock waves.

IN DILUTE PLASMAS IN THE UNIVERSE, THE USUAL TWO-BODY Coulomb collisions are relatively unimportant and the behavior of charged particles is governed by collective interactions through long-range electromagnetic forces. When some dynamical energy release occurs in these plasmas, a part of the thermal population is accelerated to high energies, so that the particle distribution deviates significantly from the Maxwell-Boltzmann distribution. By studying the particle acceleration process, we can understand the detailed physics of the energy conversion process and recognize what extreme conditions are attained by particles in the system.

The latest example from astrophysical observations is the supernova explosion that occurred early in 1987 [designated SN1987A (*1*)]. Electromagnetic radiation, from radio waves to gamma rays, as well as a neutrino burst have been detected. Astrophysicists are anxious to detect new signals, which are either directly or indirectly related to the particle acceleration processes, such as acceleration at the supernova shock wave, stochastic acceleration in the turbulence generated in the supernova ejecta, or acceleration by the strong pulsar electric field. Astrophysical observations, however, are remote-sensing observations. In the foreseeable future, we will not be able to make in situ observations of shock waves from supernovae. Because physics is an experimental science, we need a laboratory in which we can test basic principles. In this respect, the heliosphere, within which the solar wind plasma has the greatest influence on the dynamics and the energetics of particles, can be considered as a laboratory for particle acceleration processes. Of course, the parameter regime that we can reach in heliospheric observations is rather limited. Nevertheless, in this way we can learn much about the elementary principles that govern particle acceleration processes.

Let us start with an elementary consideration of the motion of charged particles in cosmic plasmas permeated by magnetic fields. Charged particles are most efficiently accelerated by the electric field, and the effects of other forces, such as gravity, are negligible. However, the electric field does not always accelerate these particles freely if the background plasma is steady and homogeneous: $\mathbf{E}_\perp$, the electric field component perpendicular to the magnetic field, $\mathbf{B}$, can only produce $\mathbf{E}_\perp \times \mathbf{B}$ drift motion (that is, magnetized motion). Suppose that the magnetic field is directed toward the page and that the electric field is directed downward (Fig. 1). A particle (of mass m), which is initially at rest, makes a cycloid motion in configuration space (Fig. 1a). The average speed of this particle is

$$\mathbf{V}_\mathrm{E} = c\,\frac{\mathbf{E}_\perp \times \mathbf{B}}{|\mathbf{B}|^2} \tag{1}$$

where c is the vacuum speed of light. In velocity space, the orbit of this particle is a circle (Fig. 1b). The maximum velocity a particle can obtain is $2|\mathbf{V}_\mathrm{E}|$. The corresponding maximum energy, $2m|\mathbf{V}_\mathrm{E}|^2$, is now known as the maximum "pickup" energy. (This name is derived from the study of cometary ions. See the next section.) To accelerate this particle to energies higher than this maximum pickup energy, it is necessary to break the magnetized motion so that the particle can move along the direction of $\mathbf{E}_\perp$. In the following sections, we shall discuss stochastic acceleration processes in unsteady plasmas, in which such a breakdown becomes possible.

Another way to accelerate particles efficiently is to have an electric field component parallel to the magnetic field, $E_\parallel$. Because the magnetic field does not prevent particle acceleration along it, $E_\parallel$ can accelerate particles freely. However, $E_\parallel$ is easily short-circuited

T. Terasawa is in the Department of Geophysics, Kyoto University, Kyoto 606, Japan. M. Scholer is at the Institut für extraterrestrische Physik, Max-Planck-Institut für Physik und Astrophysik, 8046 Garching, Federal Republic of Germany.

by electrons as a result of their high mobility, unless this mobility is suppressed by one or more physical mechanisms. In auroral particle acceleration, such suppression mechanisms (double layers, electrostatic shocks, and anomalous resistivities) are quite important (*2*).

Stochastic Acceleration Around Comets

The magnetized motion must be interrupted in order to accelerate charged particles by $\mathbf{E}_\perp$. Let $U_\perp$ be the particle velocity component perpendicular to the averaged magnetic field $\mathbf{B}_0$. Because the magnetic moment $1/2mU_\perp{}^2/|\mathbf{B}_0|$ is an adiabatic invariant, some nonadiabatic process should be invoked. If extended magnetohydrodynamic (MHD) turbulence exists in the system, the adiabaticity is violated by the cyclotron resonant interaction between charged particles and waves: this interaction occurs if the condition

$$\omega - kU_\parallel = \pm\Omega \tag{2}$$

is satisfied. Here ω and k are, respectively, the frequency and wave number of the waves; $U_\parallel$ is the particle velocity component parallel to $\mathbf{B}_0$; and Ω is the cyclotron frequency of charged particles. (For simplicity, we limit the discussion to the case where MHD waves propagate parallel to $\mathbf{B}_0$.) The physical meaning of the cyclotron resonance condition is quite simple. Helical particle orbits and wave magnetic field lines (also helical) should have the same helicity and the same pitch. The choice of the + or − sign in Eq. 2 should be made on the basis of the wave helicity and the sign of particle charge. (If the waves are linearly polarized, we should decompose them into two modes of different helicities. Only one of the two modes can resonate with particles of a given charge.) The resonance condition (Eq. 2) should be exact only in the weakest limit of the turbulence. In the turbulence of a finite amplitude, the resonance can occur within a finite frequency range by resonance broadening (*3*).

When Eq. 2 is satisified, the magnetic moment is no longer conserved and inductive electric fields accompanying the MHD turbulence contribute to the particle acceleration. One more condition, however, is needed in order for stochastic acceleration to be possible. Consider the case where the waves are propagating unidirectionally (with the same phase speed, V_A, the Alfvén velocity). In a coordinate frame comoving with these waves, the particle energy is conserved because in this frame only a static, helical magnetic field line exists and the inductive electric field vanishes. This conservation rule can be written in the laboratory frame in the following form:

$$\frac{1}{2}m\left(U_\parallel - \frac{\omega}{k}\right)^2 + \frac{1}{2}mU_\perp{}^2 = \text{const.} \tag{3}$$

Equation 3 shows that particle motions are constrained on a circle in velocity space ($U_\parallel$, $U_\perp$). Therefore, the nonadiabatic behavior of particles appears as pitch-angle diffusion on this circle, where the pitch angle is defined as $\tan^{-1}(U_\perp/U_\parallel)$. For energy diffusion to occur, the existence of waves of different phase velocities is essential. If the waves are propagating parallel to the magnetic field, $\mathbf{B}_0$, this becomes possible if there exist counterstreaming wave components, namely, waves propagating with the phase velocities V_A and $-V_A$. Figure 2 shows schematically how the energy diffusion of particles occurs in the velocity space ($U_\parallel$, $U_\perp$): particles sometimes move on a circle centered on ($+V_A$, 0) and sometimes on a circle centered on ($-V_A$, 0). Under the right circumstances, a particle can be accelerated efficiently by the combined effect of the counterstreaming waves. Of course, the same process can work in the opposite direction to decelerate the particle. Because the fate of a particle is a matter of probability, the behavior of the particle in these counterstreaming waves becomes stochastic (or diffusive).

Fig. 1. Motion of a charged particle under the effect of the electric field **E** (pointing downward) and the magnetic field **B** (pointing into the paper) in (**a**) configuration space and (**b**) velocity space.

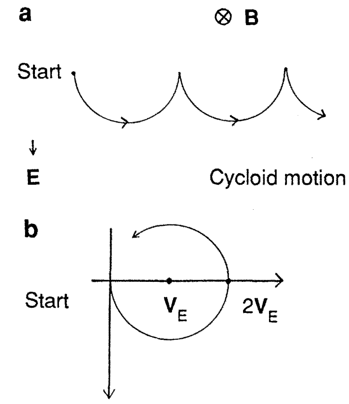

The stochastic acceleration process in a turbulent magnetic field was first proposed by Fermi (*4*). Fermi considered two types of basic interaction modes between particles and magnetic irregularities: one is reflection by a magnetic mirror ("type A"), and the other is reflection by a curved magnetic field line ("type B") (Fig. 3). The current idea of the elementary acceleration process as illustrated in Fig. 2 differs from these two types and should be categorized as the third type, "type C." There is an interesting difference between Fermi's and current ideas. In Fermi's picture, irregularities have definite velocities locally, and they accelerate or decelerate particles depending on the direction of relative motion (head-on or overtaking collisions). In the current idea, there are counterstreaming waves that coexist in the same spatial region. Particles themselves choose the interacting waves according to the resonance condition (Eq. 2) and, as a result, are scattered back and forth and stochastically accelerated.

Quantitatively, the pitch-angle scattering as well as the energy diffusion process can be treated by quasi-linear theory. For sufficiently fast particles [$U >> V_A$, where $U \equiv (U_\parallel{}^2 + U_\perp{}^2)^{1/2}$], the theory predicts that the pitch-angle diffusion occurs much faster than the energy diffusion. That is, if an anisotropic particle distribution exists initially, it will be quickly isotropized. In this limit, therefore, the behavior of the particles is well described by the isotropic distribution function $F(p,t)$, where p is the momentum of the particles, mU, and t is time. The evolution of $F(p,t)$ is governed by an energy diffusion equation (*5*),

$$\frac{\partial F}{\partial t} = \frac{1}{p^2}\frac{\partial}{\partial p}\left(p^2 D_{pp}\frac{\partial F}{\partial p}\right) \tag{4}$$

where D_{pp} is an energy diffusion coefficient. Let $P(k)$ be the power spectrum of the MHD turbulence. [$\int P(k)dk$ gives the energy density of the turbulence.] Further, let k^+ and k^- be the wave numbers of resonant waves propagating with velocities $+V_A$ and $-V_A$, respectively. Quasi-linear theory states that D_{pp} is proportional to the harmonic average of the power spectra at the resonant wave numbers, $P(k^+)$ and $P(k^-)$, namely, $2P(k^+)P(k^-)/[P(k^+) + P(k^-)]$. Note that D_{pp} vanishes for the turbulence consisting of waves propagating unidirectionally [either $P(k^+)$ or $P(k^-)$ is zero].

The stochastic acceleration process described above is realized in the neighborhood of comets. We now describe new observations obtained during the encounters with comets Giacobini-Zinner and Halley. Because of the weak gravitational force of a comet, cometary neutral gas, mainly water vapor for these comets, can escape freely from the collision-dominated inner coma. The neutral molecules from the comet are eventually ionized by photoionization by solar extreme-ultraviolet photons, charge exchange with solar wind protons, and collisional ionization by energetic electrons. After ionization, cometary ions start to move in the solar wind electromagnetic

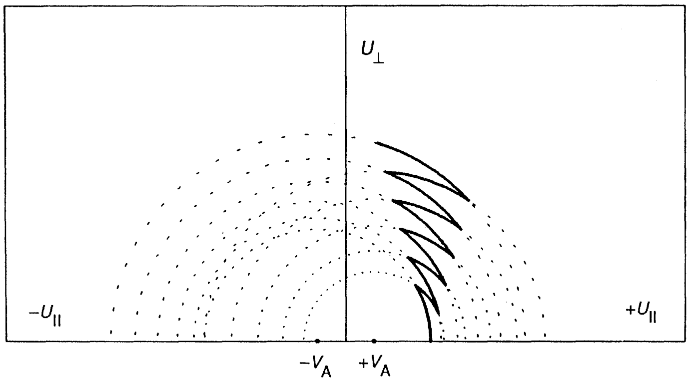

Fig. 2. Illustration of particle diffusion in velocity space. When the waves are counterstreaming with phase velocities $+V_A$ and $-V_A$, particle motion is no longer constrained on circles (dashed curves). The solid curve shows an example of the orbit of a stochastic particle.

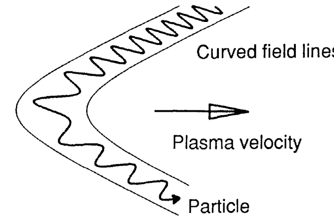

Fig. 3. Type B reflection of a particle by a curved magnetic field line. The wavy curve shows the trajectory of the particle.

field, **E** and **B** (which is called the ion pickup process). Because the outflowing velocity of parent molecules (several kilometers per second) is negligible in comparison with the **E** × **B** drift velocity in the solar wind (several hundreds of kilometers per second), the simple picture in Fig. 1 is a good approximation of the behavior of cometary ions immediately after their ionization. As time goes on, cometary ions accumulate and form a torus in velocity space. Such a torus distribution is unstable to the excitation of MHD waves that satisfy the cyclotron resonance condition (Eq. 2). Quasi-linear theory predicts that the cometary ions in the MHD waves of their own making are subjected first to the pitch-angle scattering process and next to the energy diffusion process (*6*).

In the neighborhood of Halley's comet, the result of the pitch-angle scattering was actually observed as a shell structure in velocity space, which is now called the "pickup shell" (*7, 8*). Figure 4 shows the two-dimensional velocity space distribution within the ecliptic plane for ions around Halley's comet [observed by the Suisei spacecraft (*7*)], where a color code (black-blue-green-yellow-red) shows the phase space density (in the logarithmic scale of $\sec^3/\mathrm{m}^6$). The horizontal arrow corresponds to the sunward flow direction, and the vertical arrow points toward the "eastward" flow direction. The coordinate system in Fig. 4 is the comoving frame of the spacecraft, which has a relative velocity of ≈70 km/s with respect to Halley's comet. The velocity scale is given below the color-coded distribution function. In this figure, the pickup shell of cometary water-group ions appears as a red ring. A dashed circle shows the theoretical position of the shell. As seen in Fig. 4, the agreement between expectation and observation is good. Although Fig. 4 covers only a part of the ion distribution within the ecliptic plane, results obtained with the Giotto plasma instrument, which has a three-dimensional coverage, demonstrate that these cometary ions have shell structures (*8*).

The interaction of the ions with the MHD turbulence leads to energy diffusion, so that the velocity space shell of the cometary ions eventually diffuses out. However, because newly ionized ions are continuously being injected, the shape of the pickup shell is maintained in spite of the energy diffusion. The products of the energy diffusion are more energetic ions, whose energy considerably exceeds the maximum pickup energy, $2m|\mathbf{V}_E|^2$ (several tens of kiloelectron volts for water-group ions, O^+, OH^+, and H_2O^+). The presence of ions of energies higher than 100 keV is confirmed by the observation and is interpreted in terms of the stochastic acceleration process (*9*).

The acceleration efficiency (the energy diffusion coefficient) is determined by the power spectrum of the turbulence at the resonant wavelength. Because the power spectrum of the turbulence was also observed, a more quantitative comparison between the observations and the theoretical model can be made. Figure 5 shows the power spectra of the magnetic field component transverse to $\mathbf{B}_0$, which were observed by the magnetometer on Giotto (*10*). Figure 5, a and d, shows the spectra obtained around the inbound and outbound bow shock crossings; Fig. 5, b and c, shows the power spectra in the cometosheath. The dashed lines indicate quiet solar wind spectra. As seen in these panels, the amplitude of turbulence around the comet is higher than that in the quiet solar wind by two or three orders of magnitude. The spectra shown in Fig. 5 can be well described by a power law $P(f) \propto f^{-\alpha}$ in the frequency range $f = 5$ to 300 mHz with a power law index $\alpha = 1.8$ to 2.1. Because the MHD turbulence is convected by the super-Alfvénic solar wind flow, the horizontal scale (in the unit of observed frequency f) can be readily converted to the wave number unit with the relation $k \approx 2\pi f/V_{sw}$ (where V_{sw} is the solar wind velocity). In Fig. 5b the frequency range that satisfies the cyclotron resonance condition (Eq. 2) with the water-group ions (of 0° pitch angle) is indicated by an arrow pointing to $f_{H_2O^+}$ (5 to 10 mHz).

In constructing a comprehensive model of the acceleration process of the cometary ions, we should take into account several physical effects: the spatial variation of the turbulence spectrum, the spatial variation of the ionization (injection) rate Q, and the convection effect by the solar wind flow after pickup. For example, Q falls off as $\sim(1/r^2)\exp(-r/\lambda)$, where r is the distance from the cometary nucleus and λ is the characteristic scale length for the ionization process ($\sim 10^6$ km). Therefore, we should solve, instead of the simple diffusion equation (Eq. 4), the modified equation

$$\frac{\partial F}{\partial t} + \mathbf{V}_{sw} \cdot \nabla F = \frac{1}{p^2}\frac{\partial F}{\partial p}\left[p^2 D_{pp}\frac{\partial F}{\partial p}\right] + Q \qquad (5)$$

for $F(\mathbf{x}, p, t)$, where $\mathbf{x}$ are configuration space coordinates. Gombosi solved Eq. 5 in order to compare the theoretical model with the observation near Halley's comet (*11*). In estimating D_{pp} Gombosi assumed that cometary waves propagate bidirectionally with equal amplitudes $[P(k^+) = P(k^-)]$, because the propagation direction of the turbulent waves was not measured. Therefore, his estimation corresponds to the maximal acceleration efficiency for a given total amplitude of turbulence.

In Fig. 6, calculated distribution functions $F(\mathbf{x}, p, t)$ at several values of x (distance from the cometary nucleus along the sun-comet line) are plotted against the particle energy. The stochastic Fermi process can evidently produce highly energetic ions (~300 keV for O^+). The calculated results reproduce well the characteristic shape of the observed energy spectrum (for example, the quasi-exponential shape and the characteristic energy). The diamonds represent the values observed by the Vega 1 spacecraft immediately before the bow shock crossing. The solid curve, which corresponds to the energy spectrum expected around the subsolar bow shock, is in agreement with this Vega observation.

Gombosi pointed out, however, an important quantitative differ-

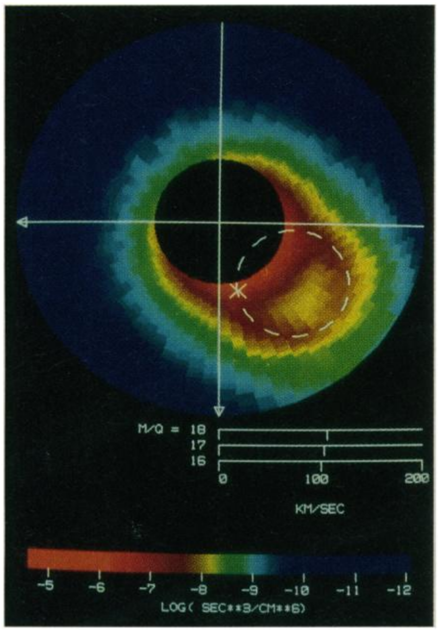

Fig. 4. An ecliptic cross section of the velocity space distribution of cometary water-group ions, O^+, OH^+, and H_2O^+. This observation was made by the Suisei spacecraft at a distance of 1.5×10^5 km from the nucleus of comet Halley. The cross marks the phase-space position where newly ionized ions first appear. A dashed circle shows the expected phase-space position of the pickup shell. The shell structure is masked by the proton contribution in the low-velocity part ($\lesssim$100 km/s). [Adapted from (7) with permission of the American Geophysical Union, Washington, DC]

ence. The energy spectra plotted in Fig. 6 are calculated along the sun-comet line, where we expect that the source term and the acceleration efficiency are maximal. On the other hand, because the trajectory of Vega is almost perpendicular to this line, the expected values of $F(\mathbf{x}, p, t)$ at the position of Vega should be much smaller (by about an order of magnitude) than those plotted in Fig. 6. What we need is some additional acceleration effect. Furthermore, it is not clear to what extent the bidirectionality of the cometary waves is realized. If the cometary waves are not bidirectional, the actual efficiency of the stochastic Fermi acceleration is less than what is assumed, so that the need for an additional acceleration process is even greater.

As a possible acceleration effect, Gombosi suggested the first-order Fermi acceleration working at the cometary bow shock. This acceleration process, which is more efficient than the stochastic Fermi acceleration process if the shock is strong enough, is discussed below. Another possibility is a nonlinear effect in the particle scattering process. In MHD turbulence of a sufficiently high level (energy density >60% of $|\mathbf{B}_0|^2/8\pi$), the nonresonant wave components (that is, the components that do not satisfy the cyclotron resonance condition, Eq. 2) do contribute to the pitch-angle scattering nonlinearly and raise the energy diffusion rate (*12*). It is interesting to see how this effect, which is not taken into account in the estimation of D_{pp} in Gombosi's calculation, could contribute to resolving the discrepancy between the measured and calculated results.

Stochastic Acceleration at Shocks

Stochastic acceleration in MHD turbulence involves accelerating as well as decelerating effects, each of which has an efficiency proportional to the velocity ratio V_A/U (where U is the velocity of particles). Because the two effects cancel each other to the first order, the net acceleration efficiency is of the order of $(V_A/U)^2$, which is small, especially for high-energy particles ($V_A/U \ll 1$). More efficient acceleration, which is of the first order of the velocity ratio, can occur around shock fronts. This process is called diffusive or first-order Fermi acceleration. Diffusive shock acceleration is caused by multiple and approximately elastic scattering of the particles in the frame of the medium upstream and downstream of a shock. The elastic scattering is the result of small-angle, pitch-angle scattering by MHD waves (see above).

The geometry around the shock is illustrated in Fig. 7. The background plasmas flow with bulk velocities $\mathbf{V}_1$ (upstream) and $\mathbf{V}_2$ (downstream) relative to the shock; V_{1n} and V_{2n} are velocity components parallel to the shock normal. We define the local Alfvén velocities in the upstream and downstream regions as V_{A_1} and V_{A_2}. Further, let $V_{A_{1,2n}}$ be the normal components of the Alfvén velocities, namely, $V_{A_{1,2}} \cos \Theta_{Bn1,2}$, where $\Theta_{Bn1,2}$ are the angles between the local magnetic fields and the shock normal direction. Because the inequalities $V_{A_{1n}} < V_{1n}$ and $V_{A_{2n}} < V_{2n}$ hold for fast shock waves (*13*), the MHD waves convect approximately with the fluid velocity. The particles that are scattered back toward the shock in the upstream medium gain energy in the shock frame; the particles that are scattered back by downstream waves lose energy. Because the flow velocity downstream of a shock is slower than that in the upstream region, the particles will end up with a positive energy gain. The prerequisite for first-order Fermi acceleration is therefore a shock with some compression ratio $R = V_{1n}/V_{2n}$ (>1) and sufficient power in the MHD waves so that the particles are scattered many times between the upstream and downstream regions.

The scattering can be described by the diffusion-convection equation for the particle distribution function $F(\mathbf{x}, p, t)$ (*14*). For an infinite planar shock and a magnetic field parallel to the shock normal (x direction), namely, for a shock with $\Theta_{Bn} = 0°$, the diffusion-convection equation reads:

$$\frac{\partial F}{\partial t} + V\frac{\partial F}{\partial x} - \frac{\partial}{\partial x}\kappa\frac{\partial F}{\partial x} - \frac{p}{3}\frac{\partial V}{\partial x}\cdot\frac{\partial F}{\partial p} = Q \qquad (6)$$

The second term on the left-hand side describes convection of the particles with the plasma flow, and the third term describes spatial diffusion by the scattering in MHD waves. Here, κ is the spatial diffusion coefficient, which is inversely proportional to the weighted

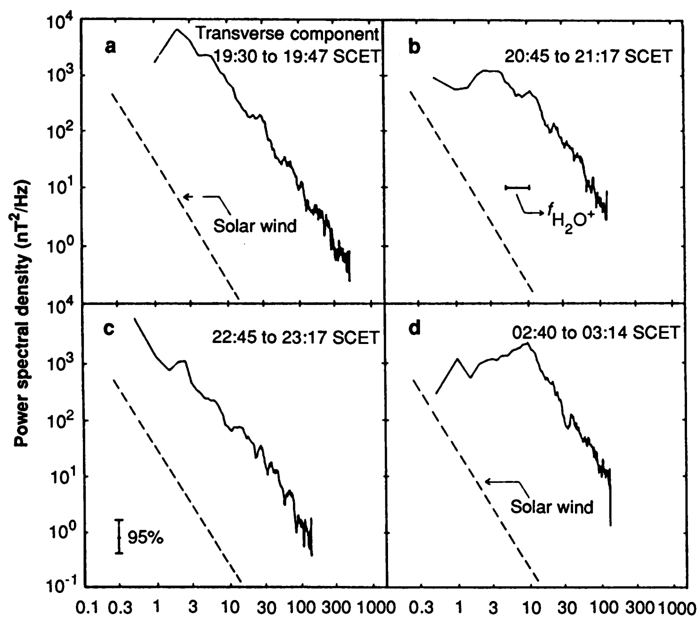

Fig. 5. Power spectra of the transverse magnetic field component for four different intervals (**a–d**) covering the inbound and outbound bow shocks as well as the cometosheath of comet Halley. The dashed lines indicate typical solar wind spectra; SCET, spacecraft event time. [Adapted from (*10*) with permission of *Astronomy and Astrophysics*]

sum of the power spectral amplitudes at the resonant wave numbers, $k^+P(k^+) + k^-P(k^-)$; k^+ and k^- correspond to the wave numbers at which the cyclotron resonance occurs (see above). The last term on the left-hand side describes the shock acceleration process. Because $\partial V/\partial x$ is nonzero through the shock (different velocities upstream and downstream), there is a transport of F in momentum space. Q is the rate at which source particles are injected into the acceleration process. In the simple case of monoenergetic injection at some momentum p_0, the steady-state solution for an infinite planar shock is a power law for F, $F \propto p^{-\beta}$, with a spectral exponent given by $\beta = 3R/(R-1)$. The corresponding differential intensity $j = dJ/dE$ is then given by $j \propto E^{-\gamma}$, where $\gamma = (R+2)/[2(R-1)]$ in the nonrelativistic regime and $\gamma = (R+2)/(R-1)$ in the relativistic regime. For strong shocks $R = V_{1n}/V_{2n}$ is close to 4, so that the spectral exponent becomes ≈ 2.

So far, the spatial diffusion coefficient has been assumed ad hoc. However, the behavior of the MHD waves is intrinsically coupled to that of the diffuse ions: the diffuse ions stream relative to the upstream plasma in the upstream direction with a bulk velocity greater than the upstream Alfvén velocity and are therefore subject to the MHD streaming instability, the threshold of which is the Alfvén velocity. This instability results in the growth of resonant MHD waves at (ω, k) that satisfy Eq. 2. The wave intensity, I, satisfies a wave kinetic equation

$$\frac{\partial I}{\partial t} + (V \pm V_A)\frac{\partial I}{\partial x} = 2\gamma I \qquad (7)$$

where γ is the growth rate of the wave amplitude and the plus sign is used for waves propagating parallel (minus sign for waves propagating antiparallel) to the bulk plasma velocity V. The growth rate γ depends on the particle pitch-angle distribution. In the limit of nearly isotropic pitch-angle distribution, γ becomes a function of S, $\gamma(S)$, where S is the particle streaming in the solar wind frame, $S = -\kappa\partial F/\partial x$. The excited waves then scatter the particles to isotropy, thus reducing the growth rate. The particles are scattered ultimately in a wave field of their own making. The spatial diffusion coefficient κ, on the other hand, is a function of the wave intensity, $\kappa = \kappa(I)$. Thus, Eqs. 6 and 7 are intrinsically coupled. Steady-state theory of this coupled behavior predicts not only the spectral form of the distribution function but also the power in the MHD waves.

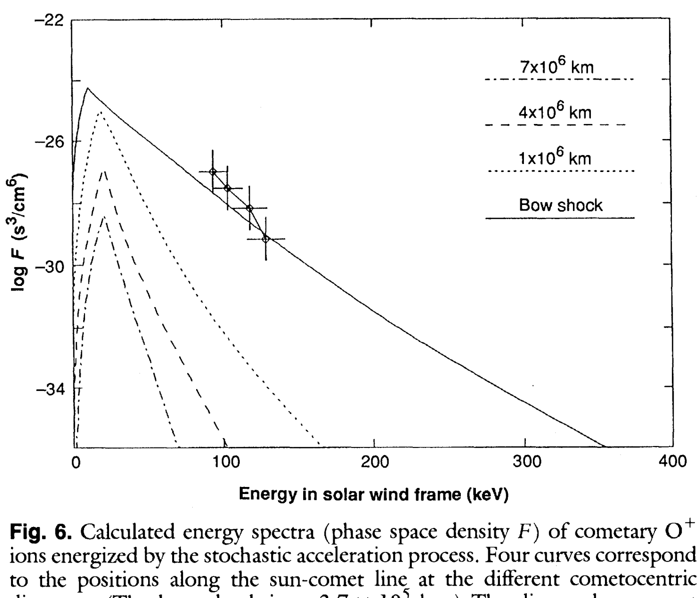

Fig. 6. Calculated energy spectra (phase space density F) of cometary O^+ ions energized by the stochastic acceleration process. Four curves correspond to the positions along the sun-comet line at the different cometocentric distances. (The bow shock is at 3.7×10^5 km.) The diamonds represent observations made by the Vega 1 spacecraft. [Adapted from (*11*) with permission of the American Geophysical Union, Washington, DC]

Fig. 7. Geometry around the shock front. The plasma bulk velocities, $\mathbf{V}_1$ and $\mathbf{V}_2$, are defined in the rest frame of the shock front. Θ_{Bn} is the angle between the shock normal and the upstream magnetic field line.

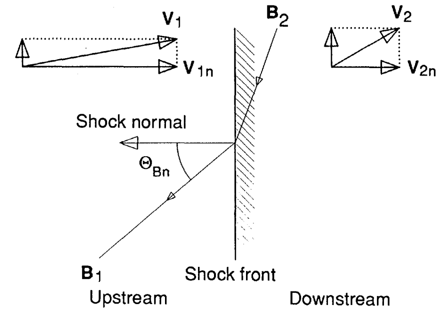

Because it has been proposed that diffusive shock acceleration of galactic cosmic rays can occur very efficiently as the result of supernova remnant shocks in the interstellar medium (*15*), it is of great importance to study and verify this process by in situ measurements in interplanetary space. The shocks available are planetary bow shocks, the so-called corotating shocks produced by the interaction of high- and low-velocity solar wind streams and the interplanetary traveling shocks produced in the course of solar mass ejections. The most detailed studies on the shock properties have been made about the terrestrial bow shock. From these studies, it is now established that the angle between the upstream magnetic field and the shock normal, Θ_{Bn} (see Fig. 7), critically controls the shock structure (*16*).

When the shock is quasi-perpendicular ($\Theta_{Bn} \gtrsim 45°$), the jumps in plasma parameters (velocity, density, magnetic field, and temperature) occur abruptly at a thin shock front, whose width is of the order of the cyclotron radius of thermal ions. When the shock is quasi-parallel ($\Theta_{Bn} \lesssim 45°$), these jumps occur in a much broader region, where there are large-amplitude fluctuations of the electromagnetic fields. The latter type of shock has been considered as the place where the first-order Fermi process works. The "diffuse ions," the nearly isotropic ions of energy 30 to 200 keV/Q observed in the quasi-parallel part of the earth's bow shock, are interpreted as products of the first-order Fermi process.

The physical environment around the earth's bow shock, however, is not simple. Because the earth's bow shock is not planar, Θ_{Bn} changes over the bow shock surface. If the interplanetary magnetic field is in the direction of the Archimedean spiral, each field line starts to connect with the dusk-side bow shock, where the shock is quasi-perpendicular. Within a few minutes, as this field line is convected further by the solar wind flow, the connection point moves toward the dawn side where the shock becomes quasi-parallel. Therefore, it is not clear to what extent diffuse ions observed at quasi-parallel bow shocks are a true quasi-parallel feature. The large-scale interplanetary shocks, where Θ_{Bn} is constant over a wide area of the shock front, are therefore expected to be much cleaner laboratories for the study of shock acceleration. Corotating shocks usually build up in the outer solar system, that is, beyond 1 astronomical unit (AU). Because there are relatively few space probes exploring the outer solar system, most information on shock acceleration comes from the traveling interplanetary shocks observed close to 1 AU.

A detailed comparison of the measurements collected for a quasi-parallel shock and the self-consistent theory (*17*) for the excitation of MHD waves and the diffusive acceleration has been performed by Kennel *et al.* (*18*). This shock was observed by the International Sun-Earth Explorer-3 spacecraft on 12 November 1978 at a distance of ~ 220 earth radii in front of the earth's bow shock. Figure 8a shows the proton intensity in three energy channels as a function of time. In the middle and highest energy channels, there was an enhanced number of energetic particles present in interplanetary space before the shock arrival on 12 November 1978. These are solar flare–

produced particles. However, shortly before the shock arrival, the intensity in the energy range below ~300 keV shows an increase of almost two orders of magnitude. These are the interplanetary shock–accelerated protons, which exhibit the typical intensity-time profile: a sharp increase starting before shock arrival and an almost constant intensity in the postshock regime. The short-lived spikes observed in the lowest energy channel well before shock arrival are energetic protons accelerated at the earth's bow shock; these spikes are observed whenever the interplanetary magnetic field lines connect the spacecraft position with the earth's bow shock. Figure 8b shows three trace magnetic field spectra computed for 2.5-min segments of data beginning 12.5, 7.5, and 2.5 min before the shock passed over the spacecraft. These data show the correlation between the proton intensity increase and the total power in the MHD waves as the shock approaches the spacecraft. The self-consistent theory predicts the relation between the integrated wave amplitude and the total energy density in the shock-accelerated protons. This prediction proved to be very close to the observed one.

As theory also predicts, a power-law energy spectrum of accelerated particles was observed. As far as the theoretical spectral exponent is concerned, we would like to make a further comment: the compression ratio R in the expression of the spectral exponent should more exactly be $(V_{1n} - V_{1n}^*)/(V_{2n} - V_{2n}^*)$, where V_{1n}^* and V_{2n}^* are normal components of the propagation velocities of resonant waves defined in the local rest frames of the upstream and downstream plasmas. In the simple case of the parallel shock ($\Theta_{Bn} = 0°$), they would be $\pm V_{A_1}$ and $\pm V_{A_2}$, where the proper sign should be chosen according to the wave propagation direction. However, we should take into account the possibility that the waves are not purely Alfvénic and have propagation velocities different from $\pm V_A$: if the shock is oblique, magnetic perturbations can propagate with the speeds of the fast or slow magnetosonic waves. Furthermore, if the downstream plasma has an enhanced pressure anisotropy, the phase velocities of the MHD waves are greatly modified. In spite of these problems, Kennel *et al.* found good agreement between the theoretical and observed values of the spectral exponent by taking

$$R = (V_{1n} - V_{A_1n})/(V_{2n} - V_{A_2n}) \tag{8}$$

Because the propagation direction of the waves was not determined observationally, it has not yet been demonstrated that this expression for R is appropriate. Indeed, Tan *et al.* (*19*) reported cases where the spectral exponents from Eq. 8 do not agree with the observation. In future studies of the acceleration process, it will be important to investigate the nature of the turbulence around shocks.

Another important question is whether a shock can accelerate ions directly out of the thermal plasma population (solar wind) or whether there must be a preaccelerated particle population, such as solar flare particles, which are then further accelerated by the shock. This question cannot be answered from proton measurements at interplanetary traveling shocks alone, because almost all strong, interplanetary traveling shocks that are accompanied by significant particle acceleration events are produced in the course of solar flares and thus invariably come with flare particles. However, by comparing the relative abundances of various ionic species in the solar wind, in the flare population, and in the shock-accelerated population, investigators have begun to address this question. Weak interplanetary shocks are produced by nonflare coronal mass ejection (CME) events without accompanying solar particles. However, acceleration at these shocks is usually not efficient enough to produce significant particle events.

It has been shown (*20*) that the density ratio of protons to alpha-particles in the solar wind correlates very well with the proton-to-alpha particle flux ratio (at ~40 keV) of particles accelerated by interplanetary, traveling shocks. A similar result has been shown for the earth's bow shock (*21*). These findings strongly indicate that at interplanetary traveling shocks as well as at planetary bow shocks

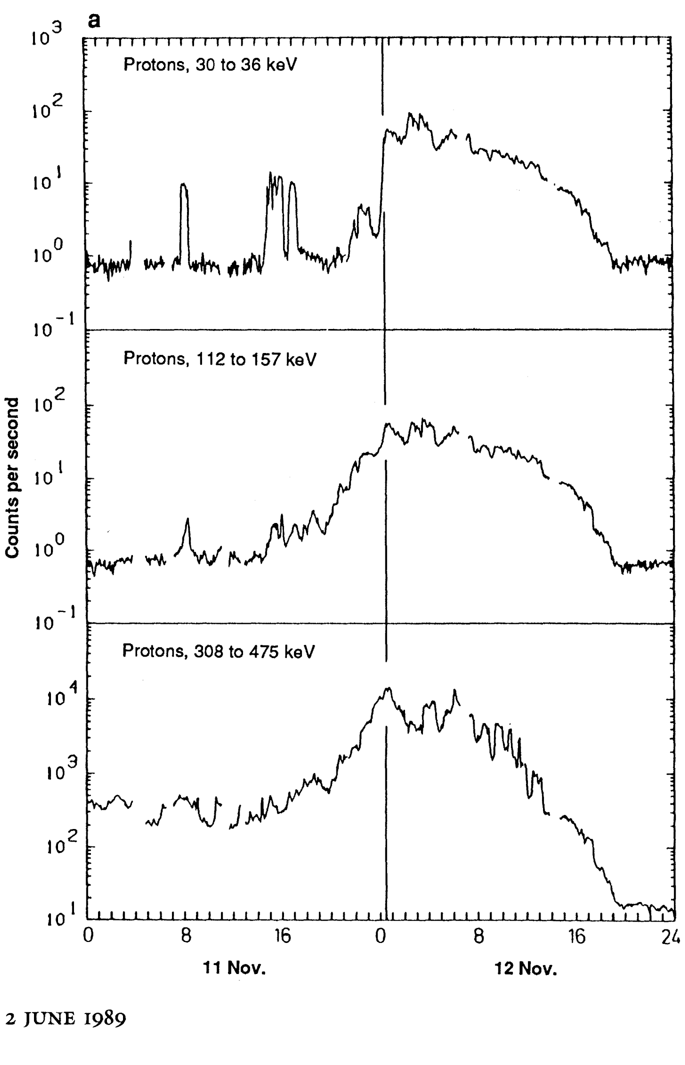

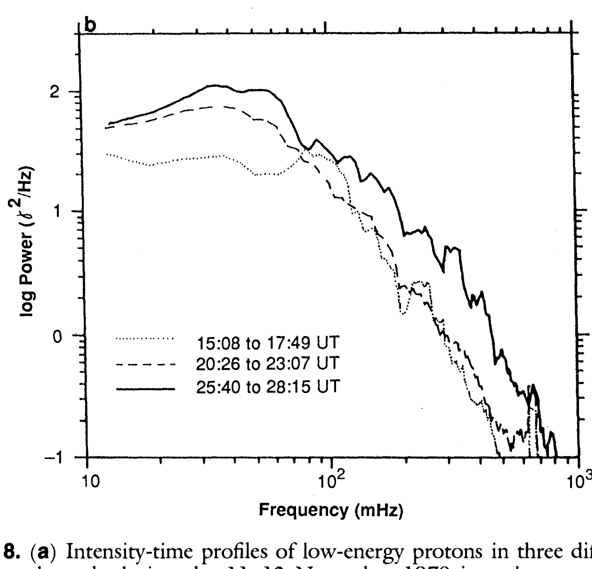

Fig. 8. (**a**) Intensity-time profiles of low-energy protons in three different energy channels during the 11–12 November 1978 interplanetary shock event. The solid line shows the time of shock passage. (**b**) Upstream wave power spectra near the shock, drawn in three different 2.5-min data segments. The last segment ended 1 s before the shock arrival. [Adapted from (*18*) with permission of the American Geophysical Union, Washington, DC]

ions are directly accelerated out of the thermal plasma population. At higher energies (>200 keV) the flare-accelerated particles are the main seed population for shock acceleration at the interplanetary traveling shocks.

One more piece of evidence in support of the idea that the thermal plasma is a source of seed particles for shock acceleration comes from recent measurements of ions upstream of the earth's bow shock (*22*). Figure 9 shows energy per charge of H^+, He^{2+}, and CNO during an energetic particle event upstream of the bow shock. The proton spectrum has been composed from measurements obtained with two different instruments, an energetic particle detector and a plasma instrument on the AMPTE/IRM spacecraft (Active Magnetospheric Particle Tracer Experiment/Ion Release Module). It thus covers an energy range from ~200 eV to ~80 keV. The proton spectrum exhibits two different components: a solar wind distribution with a peak close to ~1 keV, corresponding to the solar wind bulk flow velocity, and a second, higher energy upstream population between ~3.5 and ~80 keV, which is identified as diffuse protons on the basis of their angular distribution. The spectrum of the diffuse protons emerges smoothly out of the solar wind thermal distribution and extends continuously over more than six decades in differential flux (Fig. 9). This indicates one source for the diffuse ions over the whole energy range, namely, the solar wind.

Above ~200 keV the spectrum of diffuse bow shock ions exhibits a sharp intensity decrease. Such a decrease can be the result of various effects (*23*): the acceleration time is limited because of the limited connection time of the interplanetary magnetic field and the bow shock; the large mean free path of high-energy particles leads to free escape in the upstream direction; because of diffusion across magnetic field lines, high-energy particles are lost to the flanks of the bow shock. The spectrum of energetic particles associated with interplanetary traveling shock also exhibits at 1 AU a deviation from a power law above ~500 keV, a result of the fact that above this energy the diffusive acceleration process at a quasi-parallel shock is not yet in a steady state. Diffusive acceleration at a quasi-parallel shock is not an immediate process, because a particle has to cross the shock many times in order to pick up an appreciable amount of energy. At 0.5 MeV, the characteristic acceleration time τ is about 35 hours and therefore is of the same order of magnitude as the shock travel time from the sun to 1 AU (*24*). Above this energy, the diffuse population is not in a steady state and a power-law spectrum cannot be expected.

The characteristic time τ for acceleration of particles from an initial momentum p_0 to a momentum p_1 is (*25*)

$$\tau = \frac{3}{V_{1n} - V_{2n}} \int_{p_0}^{p_1} \left(\frac{\kappa_1}{V_{1n}} + \frac{\kappa_2}{V_{2n}} \right) \frac{dp}{p} \tag{9}$$

Because $\kappa_{1,2}$ are tensors of the second rank, they can be represented in terms of the diffusion coefficients parallel and perpendicular to the magnetic field as $\kappa_{1,2} = \kappa_{\parallel 1,2}\cos^2(\Theta_{Bn1,2}) + \kappa_{\perp 1,2}\sin^2(\Theta_{Bn1,2})$.

We usually have the relation that $\kappa_\parallel >> \kappa_\perp$, unless the MHD turbulence is so strong that the mean free path of particles becomes as short as their cyclotron radius. Therefore, with the same power in the MHD turbulence, the acceleration efficiency increases (τ decreases) with increasing $\Theta_{Bn} \rightarrow 90°$. This means that diffusive acceleration to high energies proceeds faster at more quasi-perpendicular shocks (*26*). The physical reason for the increased acceleration rate at quasi-perpendicular shocks is as follows. The acceleration term in Eq. 6 is proportional to $dp/dt \equiv -(p/3)\text{div}\mathbf{V}$, which can be separated into two parts,

$$-\frac{p}{3}\text{div}\mathbf{V} = -\frac{p}{3}\text{div}\mathbf{V}_\parallel \; -\frac{p}{3}\text{div}\mathbf{V}_\perp \tag{10}$$

where $\mathbf{V}_\parallel$ is the component of plasma flow velocity parallel ($\mathbf{V}_\perp$ is

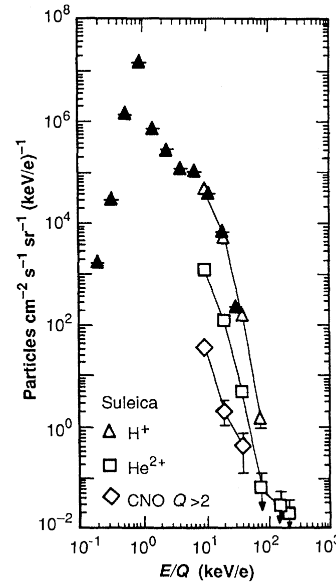

Fig. 9. Averages (20 min) of the H^+, He^{2+}, and CNO ($Q \approx 6$) energy spectra in energy per charge unit observed by the AMPTE/IRM spacecraft, 5 September 1984, 03:00 to 03:20 UT. The peak of the spectrum (~1 keV/Q) for H^+ (▲) represents the solar wind kinetic energy. [Adapted from (*22*) with permission of the American Geophysical Union, Washington, DC]

the component perpendicular) to the local magnetic field. The first part, $-(p/3)\text{div}\mathbf{V}_\parallel$, gives the energy change due to compression. The second part, $-(p/3)\text{div}\mathbf{V}_\perp$, represents the energy change due to magnetic gradient drift in the $-\mathbf{V} \times \mathbf{B}$ electric field (*27*). As Θ_{Bn} approaches 90°, the effect of the drift motion on the acceleration process becomes quite important and the acceleration efficiency increases (or τ decreases). If the turbulence is absent in the case of oblique shocks ($\Theta_{Bn} < 90°$), only the drift effect remains. This is the so-called "shock drift acceleration" process [see (*28*)]. The degree of scattering, which constitutes the distinction between these two different acceleration processes, differs from event to event and is a focus of ongoing debate on the interpretation of observed acceleration events in interplanetary space (*29*).

Summary and Comment

We have discussed the basic physics of particle acceleration processes in which the vital interaction between particles and MHD turbulence plays an essential role. In both cases discussed here, stochastic acceleration around comets and stochastic shock acceleration, the particles interact during their acceleration with an MHD turbulent wave field of their own making. Therefore, the problem is highly nonlinear in nature. Although the quasi-linear approach has been successfully used in studying the acceleration processes, nonlinearities that are not included in the quasi-linear treatment often have considerable consequences. Possible nonlinear enhancement of the acceleration rate discussed in the context of the cometary particles is an example. It remains for future investigators to delineate the physics of particle acceleration processes in the full light of their nonlinearity.

We have also addressed the problem of source particles, namely, the "raw material" for the acceleration processes. In the case of cometary ions, this is a simple problem: all cometary ions newly ionized in the solar wind are injected into the stochastic acceleration process. In the case of the shock-accelerated ions, on the other hand, the problem is not so easy. We have shown evidence that out of the thermal plasma population some particles are accelerated to much higher energy. In spite of recent developments in our understanding of the physics of collisionless shock waves (*30*), there is much to be done, both experimentally and theoretically, if we are to understand the process by which the source particles are chosen from the majority of thermal particles.

REFERENCES AND NOTES

1. S. E. Woosley and M. M. Phillips, *Science* **240**, 750 (1988).
2. C. Cattell, *Geophys. Monogr. Am. Geophys. Union* **28**, 304 (1984); R. A. Smith, in *Unstable Current Systems and Plasma Instabilities in Astrophysics*, M. R. Kundu and G. D. Holman, Eds. (Symposium **107**, Reidel, Dordrecht, 1985), pp. 113–123.
3. T. H. Dupree, *Phys. Fluids* **9**, 1773 (1966); H. J. Völk, *Astrophys. Space Sci.* **25**, 471 (1973).
4. E. Fermi, *Astrophys. J.* **75**, 1169 (1949).
5. J. Skilling, *Mon. Not. R. Astron. Soc.* **172**, 557 (1975); J. G. Luhmann, *J. Geophys. Res.* **81**, 2089 (1976).
6. W.-H. Ip and W. I. Axford, *Planet. Space Sci.* **34**, 1061 (1986); P. A. Isenberg, *J. Geophys. Res.* **92**, 1067 (1987); B. E. Gribov *et al.*, *Astron. Astrophys.* **187**, 293 (1987).
7. T. Mukai *et al.*, *Geophys. Res. Lett.* **13**, 829 (1986).
8. M. Neugebauer *et al.*, *Nature* **321**, 352 (1986); *Astron. Astrophys.* **187**, 21 (1987).
9. G. D. Gloeckler *et al.*, *Geophys. Res. Lett.* **13**, 251 (1986); R. J. Hynds, S. W. H. Cowley, T. R. Sanderson, K.-P. Wenzel, J. J. Van Rooijen, *Science* **232**, 361 (1986); S. McKenna-Lawlor *et al.*, *Nature* **321**, 347 (1986); A. J. Somogyi *et al.*, *ibid.*, p. 285; I. G. Richardson *et al.*, *Planet. Space Sci.* **35**, 1323 (1987).
10. K. H. Glassmeier *et al.*, *Astron. Astrophys.* **187**, 65 (1987).
11. T. M. Gombosi, *J. Geophys. Res.* **93**, 35 (1988).
12. T. Terasawa, *Geophys. Monogr. Am. Geophys. Union*, in press.
13. A. Jeffery and T. Taniuti, *Nonlinear Wave Propagation with Application to Physics and Magnetohydrodynamics* (Academic Press, New York, 1964), chap. 6, pp. 219–238.
14. The original form of the diffusion-convection equation was derived by E. N. Paker, *Planet. Space Sci.* **13**, 9 (1965).
15. W. I. Axford, E. Leer, G. Skadron, *Proc. 15th Int. Conf. Cosmic Rays* **11**, 132 (1977); R. D. Blandford and J. P. Ostriker, *Astrophys. J.* **221**, L29 (1978); A. R. Bell, *Mon. Not. R. Astron. Soc.* **182**, 147 (1978).
16. E. W. Greenstadt, *Geophys. Monogr. Am. Geophys. Union* **35**, 169 (1985).
17. M. A. Lee, *J. Geophys. Res.* **88**, 6109 (1983).
18. C. F. Kennel *et al.*, *ibid.* **91**, 11917 (1986).
19. L. C. Tan *et al.*, *ibid.* **93**, 7225 (1988).
20. L. C. Tan *et al.*, *ibid.* **91**, 11009 (1986).
21. F. M. Ipavich, J. T. Gosling, M. Scholer, *ibid.* **89**, 1501 (1984).
22. E. Möbius *et al.*, *Geophys. Res. Lett.* **14**, 681 (1987).
23. M. Scholer, F. M. Ipavich, G. Gloeckler, D. Hovestadt, *J. Geophys. Res.* **85**, 4602 (1980); D. Eichler, *Astrophys. J.* **244**, 711 (1981).
24. B. Klecker *et al.*, *Astrophys. J.* **251**, 393 (1981).
25. G. E. Morfill *et al.*, *ibid.* **246**, 810 (1981); L. Drury, *Rep. Prog. Phys.* **46**, 973 (1983); P. O. Lagage and C. J. Cesarsky, *Astron. Astrophys.* **125**, 249 (1983).
26. J. R. Jokipii, *Astrophys. J.* **313**, 842 (1987).
27. J. Kota, *Proc. 16th Int. Cosmic Ray Conf.* **3**, 13 (1979); J. R. Jokipii, *Astrophys. J.* **255**, 716 (1982).
28. R. B. Decker, *J. Geophys. Res.* **88**, 9959 (1983); E. T. Sarris and S. M. Krimigis, *Astrophys. J.* **298**, 676 (1985); T. R. Sanderson *et al.*, *J. Geophys. Res.* **90**, 19 (1985).
29. M. Scholer, in *Proceedings of the Sixth International Solar Wind Conference*, V. J. Pizzo, T. Holzer, D. G. Sime, Eds. (Technical Note 306, National Center for Atmospheric Research, Boulder, CO, 1987), pp. 465–479.
30. Recent developments in the study of collisionless shocks are summarized in *Geophys. Monogr. Am. Geophys. Union* **34** (1985) and **35** (1985).
31. We are grateful to J. R. Jokipii, F. Jones, M. A. Lee, A. Nishida, and M. Fujimoto for valuable and stimulating discussions. We thank L. M. Kistler for careful reading of the manuscript. T.T. was supported by Grants-in-Aid for Scientific Research (62302011 and 62540309) from the Ministry of Education, Science, and Culture of Japan.

Research Articles

Ectopic Expression of the Serotonin 1c Receptor and the Triggering of Malignant Transformation

DAVID JULIUS, THOMAS J. LIVELLI, THOMAS M. JESSELL, RICHARD AXEL

Neurotransmitter receptors are usually restricted to neuronal cells, but the signaling pathways activated by these receptors are widely distributed in both neural and nonneural cells. The functional consequences of activating a brain-specific neurotransmitter receptor, the serotonin 5HT1c receptor, in the unnatural environment of a fibroblast were examined. Introduction of functional 5HT1c receptors into NIH 3T3 cells results, at high frequency, in the generation of transformed foci. Moreover, the generation and maintenance of transformed foci requires continued activation of the serotonin receptor. In addition, the injection of cells derived from transformed foci into nude mice results in the generation of tumors. The serotonin 5HT1c receptor therefore functions as a protooncogene when expressed in NIH 3T3 fibroblasts.

NEUROTRANSMITTERS MEDIATE RAPID INTERCELLULAR communication within the nervous system by interacting with cell surface receptors. These receptors often trigger second messenger signaling pathways that regulate the activity of ion channels. Although neurotransmitter receptors by definition have been restricted to the nervous system, their second messenger systems have been observed in both neural and nonneural cells. These observations raise the question as to the functional consequences of introducing a neurally restricted transmitter receptor into nonneural cells.

Serotonin is one example of a neurotransmitter that mediates diverse neural functions by binding to multiple receptor subtypes (*1*). Moreover, individual serotonin receptor subtypes couple to different intracellular signaling systems. The 5HT1c and 5HT2 receptors activate phospholipase C (*2*), whereas the 5HT1a and 5HT1b receptors modulate adenylate cyclase activity (*3*). In neurons that express the 5HT1c and 5HT2 receptors, receptor activation by serotonin is likely to generate inositol polyphosphates that release intracellular Ca^{2+} (*2, 4*). In other neurons that express the 5HT1a receptor, changes in cyclic adenosine monophosphate levels or activation of G proteins appears to regulate K^+ channel function (*5*).

We have recently cloned and characterized the genes encoding the 5HT1c and 5HT2 receptors (*6, 7*). These proteins are members of the family of G protein–coupled receptor molecules that traverse the membrane seven times. Introduction of the 5HT1c gene into

The authors are in the Department of Biochemistry and Molecular Biophysics, and the Howard Hughes Medical Institute, College of Physicians and Surgeons, Columbia University, New York, NY 10032.